

Physical Characteristics and Chemical Degradation of Amorphous Quinapril Hydrochloride

YUSHEN GUO,^{1*} STEPHEN R. BYRN,² GEORGE ZOGRAFI²

¹ School of Pharmacy, University of Wisconsin-Madison, Madison, WI 53706

² School of Pharmacy, Purdue University, West Lafayette, IN 47907

Received 26 July, 1999; accepted 12 November, 1999

ABSTRACT: This study was designed to investigate the relationships between the solid-state chemical instability and physical characteristics of a model drug, quinapril hydrochloride (QHCl), in the amorphous state. Amorphous QHCl samples were prepared by rapid evaporation from dichloromethane solution and by grinding and subsequent heating of the crystalline form. Physical characteristics, including the glass transition temperature and molecular mobility, were determined using differential scanning calorimetry, thermogravimetric analysis, powder x-ray diffractometry, polarizing microscopy, scanning electron microscopy, and infrared spectroscopy. The amorphous form of QHCl, produced by both methods, has a T_g of 91°C. Isothermal degradation studies showed that cyclization of QHCl occurred at the same rate for amorphous samples prepared by the two methods. The activation energy was determined to be 30 to 35 kcal/mol. The rate of the reaction was shown to be affected by sample weight, dilution through mixing with another solid, and by altering the pressure above the sample. The temperature dependence for chemical reactivity below T_g correlated very closely with the temperature dependence of molecular mobility. Above T_g , however, the reaction was considerably slower than predicted from molecular mobility. From an analysis of all data, it appears that agglomeration and sintering of particles caused by softening of the solid, particularly above T_g , and a resulting reduction of the particle surface/volume ratio play a major role in affecting the reaction rate by decreasing the rate of removal of the gaseous HCl product. © 2000 Wiley-Liss, Inc. and the American Pharmaceutical Association *J Pharm Sci* 89: 128–143, 2000

INTRODUCTION

It has been proposed previously^{1,2} that all chemical reactions in the solid state involve a number of steps that serve as activation barriers and, hence, influence the overall reactivity. These include the chemical activation energy associated with the reaction, the activation energy associated with mass transport or molecular mobility, and an activation barrier associated with nucle-

ation of any new solid phase that might occur. For most pharmaceutical degradation reactions, because of the importance of molecular mobility, reaction rates are greatest in the liquid or solution states and least in the crystalline state, with intermediate rates occurring in the amorphous state.^{3–5} Because processing of crystalline materials often leads to disorder and the introduction of fully or partially amorphous states, it would seem important to be able to link the properties of drugs in such disordered states (e.g., time scales of molecular mobility) to the time scales observed for chemical degradation.⁶

In this article we report a study of the chemical degradation of quinapril hydrochloride (QHCl) in the amorphous state as a function of temperature

*Present address: Pharmaceutical Research & Development, Meriel Limited, North Brunswick, NJ 08902

Correspondence to: G. Zografi (E-mail: gzografi@facstaff.wisc.edu)

Journal of Pharmaceutical Sciences, Vol. 89, 128–143 (2000)
© 2000 Wiley-Liss, Inc. and the American Pharmaceutical Association

and other sample-related variables. This compound represents a model molecule for both angiotensin-converting enzyme (ACE) inhibitors and a large number of HCl salt form pharmaceuticals in the solid state. In previous studies with quinapril HCl,⁷ it has been shown that the major degradation pathway in the solid state is intramolecular cyclization (aminolysis) with the formation of a diketopiperazine (DKP) compound (Scheme 1) similar to those observed for other structurally related ACE inhibitors, such as moxipril⁸ and enalapril.⁹ This type of cyclization reaction also occurs readily in some polypeptides^{10–12} and proteins.¹³ A mechanistic understanding of this reaction in the solid state could be useful in a better comprehension of their stability and the synthesis of certain types of peptides.¹⁴ Our major goal is to prepare and characterize the amorphous form of quinapril HCl and to ascertain as quantitatively as possible the extent to which the chemical reaction is affected by its amorphous characteristics through effects on molecular mobility and/or other physical properties.

MATERIALS AND METHODS

Materials

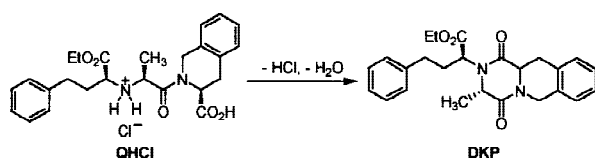
Quinapril hydrochloride, QHCl, [3*S*-[2[*R**(*R**),3*R**]]-2-[2-[[1-(ethoxycarbonyl)-3-phenylpropyl]amino]-1-oxopropyl]-1,2,3,4-tetrahydro-3-isoquinolinecarboxylic acid, hydrochloride, was a gift from the Chemical Processing Division of the Warner-Lambert Co. (Holland, MI). Crystalline quinapril HCl, as the acetonitrile solvate (QHCl-CH₃CN), was prepared by recrystallization from acetonitrile.¹⁵ Powder x-ray diffraction studies (PXRD) gave the same diffraction pattern as reported previously.⁷ The major degradation product, quinapril diketopiperazine (DKP, mp = 121–123°C), [3*S*-[2(*R**),3*α*,11-*α*β]]-1,3,4,6,11,11*α*-hexahydro-3-methyl-1,4-dioxo-*α*-(2-phenylethyl)-2*H*-pyrazino[1,2-*b*]isoquinoline-2-acetic acid, ethyl ester, and quinapril diacid (DA, mp = 166–168°C), [3*S*-[2[*R**(*R**),3*R**]]-2-[2-[[1-(1-carboxy)-3-phenylpropyl]amino]-1-oxopropyl]-1,2,3,4-tetrahydro-3-isoquinolinecarbox-

ylic acid, were prepared according to literature methods.¹⁶ Trifluoroacetic acid (99+%, spectrophotometric grade), dichloromethane (99.8% anhydrous), and FT-IR grade potassium bromide (99+%) were purchased from Aldrich Chemical Co, Inc. (Milwaukee, WI). Analytical reagent grade potassium chloride (99.85%) was obtained from Mallinckrodt Specialty Chemicals Co. (Paris, KY). Both potassium halides used for the infrared spectroscopic measurements were dried under vacuum in a desiccator with P₂O₅ before use. Water was purified by a SYBRON/Barnstead pressure cartridge system (PCS) (Boston, MA). High-performance liquid chromatography (HPLC) grade acetonitrile and methanol were purchased from EM Scientific (Gibbstown, NJ). All chemicals were used without further purification, unless otherwise specified.

Untreated glass beads and siliconized glass beads were obtained from the Ferro Corporation/Cataphote Division (Jackson, MS), with particle diameters in the range of 88 to 125 μm. They were specified by the manufacturer to contain no more than 15% irregularly shaped particles. The densities of both glass beads were determined by pycnometric measurement to be 2.47 g/cm³. The siliconized beads, with a surface covered by methyl groups, were shown to be completely nonwetted by water, whereas the untreated beads were completely wetted.¹⁷ Amorphous trehalose (T_g = 115°C) was prepared from D(+)(trehalose dihydrate (Sigma Chemical Co., St. Louis, MO) by lyophilization using a previously reported method.¹⁸

Preparation of Amorphous QHCl by Grinding of Crystalline QHCl-CH₃CN

The crystalline sample of acetonitrile solvate was ground for 10 min using a heavy-duty laboratory Wig-L-Bug (WIG-3110-3A) electric motor grinder (Spectra-Tech Inc., Stamford, CT) equipped with a timer, a fan-cooled motor, and an adapter for a stainless steel vial (1/2-inch diameter × 1 inch long) with a 1/4-inch diameter stainless steel ball. During grinding, the Wig-L-Bug has a reciprocating figure-8 action through a 6 1/2° arc at 3200 RPM; the stainless steel ball thus strikes the ends of the vial some 200 times in 1 second. After grinding, the sample was dried in a Precision Scientific Model 19 laboratory vacuum oven (Chicago, IL) at 45°C (–0.5 Torr) for 24 hours.



Preparation of Amorphous QHCl by Solvent Evaporation

QHCl was dissolved in a minimum amount of CH_2Cl_2 required to form a clear solution. The solvent was then removed in a rotary evaporator under vacuum at $\sim 30^\circ\text{C}$, and the residue was dried in a desiccator containing P_2O_5 under vacuum. After being ground for 10 seconds using the previously described Wig-L-Bug electric motor grinder, the sample was dried further in a vacuum oven at 45°C for 24 hours as already described.

Samples prepared by both methods were determined to be completely amorphous using PXRD (described later) and by the absence of birefringence under polarized light with an Olympus BH-2 optical microscope (Olympus Optical Co., LTD, Tokyo, Japan). The water content of the various samples was determined with an EM Science Aquastar C200 titrator (Cherry Hill, NJ) and found to be less than 0.1% (w/w) in all cases using a minimum of three individual samples.

Powder X-Ray Diffractometry

The powder x-ray diffraction patterns of various solid samples were determined at ambient temperature using a Scintag PadV powder x-ray diffractometer (Scintag Inc., Santa Clara, CA) at 40 mA and 35 kV with $\text{Cu K}\alpha$ radiation. Counts were measured with a scintillation counter. Samples (~ 0.5 -mm thickness) were packed onto a piece of double-sided cellophane tape on a quartz holder. The samples were scanned, with the diffraction angle, 2θ , increasing from 5° to 40° , with a step size of 0.02° and a counting time of 1 second.

High-Performance Liquid Chromatography

A Thermoste Separation Products HPLC system (Spectra-Physics Analytical, Fremont, CA) was used to separate and identify quinapril and its degradation products. It consisted of a Spectra SYSTEM P1000 pump, a Spectra SYSTEM UV1000 detector, and a ChemJet integrator. An Altex Ultrasphere-ODS reverse phase column (4.6 mm ID \times 25 cm, Alltech, Deerfield, IL) and an ODS guard column cartridge (2.0 mm ID \times 1 cm, Upchurch Scientific, Oak Harbor, WA) were used. The mobile phase consisted of a mixture of acetonitrile in water (50% v/v) with an additional 0.1% (v/v) trifluoroacetic acid. The flow rate was 1.0 ml/min, and the detection wavelength was 220

nm. Quantitative analysis is based on the response factors of peak areas relative to those obtained by measuring authentic pure samples.

Thermogravimetric Analysis

Thermogravimetric analysis (TGA) curves were obtained with a Netzsch Thermo-Microbalance TG 209 and TASC 414/3 temperature control and data acquisition system (NETZSCH Instruments Incorporated, Stamford, CT) controlled by a PC with NETZSCH TA software for data acquisition and analysis. Temperature was calibrated by the Curie point temperature of Ni (627 K). All TGA runs were performed in an open Al_2O_3 crucible (85 μl) with purge and protective nitrogen gas flow at 25 and 30 ml/min, respectively. All non-isothermal TGA experiments were performed at a heating rate of 10 K/min using 5 to 10 mg per sample.

Differential Scanning Calorimetry

The differential scanning calorimetry (DSC) thermograms for various systems were determined using a Seiko I SSC/5200 differential scanning calorimeter (Seiko Instruments, Horsham, PA) equipped with a Hewlett Packard Model 712/60 data station. Dry nitrogen was used as the purge gas (85 ml/min) and liquid nitrogen as the coolant. High-purity indium, gallium, and biphenyl were used for temperature and enthalpy calibration at different heating rates. Samples (5–10 mg) in nonhermetically crimped aluminum pans with a pinhole in the lid were heated at 5 to 30 K/min. The glass transition temperature was determined by constructing tangents to the DSC curve baselines before and after the glass transition. The intersection of these tangents to the tangent at the inflection point gives the extrapolated onset and endpoint temperatures. The onset of these temperatures is reported as the glass transition temperature. All reported values are the average of at least three independent measurements.

FT-IR Spectra

FT-IR spectra were obtained with a Galaxy Series FT-IR 5000 spectrophotometer made by ATI Mattson (Madison, WI). The IR spectrometer was controlled by a PC with WinFIRST-Fourier Infrared software for data acquisition and analysis. KCl and KBr pellets of solid samples were prepared with a mini-press without any extra grind-

ing. The weight ratio of KCl or KBr to drug was about 100.

Scanning Electron Microscopy

The surface morphology of various amorphous drug samples was investigated using a LEO scanning electron microscope (LEO Elektronenmikroskopie GmbH, D-73446 Oberkochen, Germany). The dry powder was mounted onto metal stubs using a piece of double-sided conductive adhesive tape and vacuum-coated with a platinum film using a Desk II cold sputter/etch unit (Denton Vacuum, Inc., Cherry Hill, NJ).

Solid-State Stability

The solid-state thermal degradation of QHCl was studied by placing samples of known weight (0.5–15 mg) into open 2-ml glass vials, which were then placed into a desiccator containing P_2O_5 to maintain dryness. A Fisher Scientific Isotemp® Premium Oven (Model 750G) was used to maintain constant temperature. The sample temperature was monitored using an Omega microprocessor thermometer (Model HH23) with a type-K thermocouple in direct contact with the solid sample. Samples were selected at different time intervals and dissolved in methanol before carrying out the HPLC assay. Besides the major cyclization product (DKP), the appearance of quinapril diacid (DA), the ethyl ester hydrolysis product, was also followed by HPLC analysis and shown to be very limited (i.e., a maximum of 5% of DKP product over the same period for which the cyclization reaction was followed). Consequently, the focus of this study and the discussion that follows will be on the cyclization reaction. All data analysis and curve fitting were carried out using Microcal Origin™ Version 4.1 Microcal Software Inc. (Northampton, MA).

RESULTS

Solid-State Characteristics

Thermogravimetric Analysis of Crystalline Quinapril HCl

Crystalline QHCl- CH_3CN was studied by TGA and compared with ground samples and samples heated under vacuum (Fig. 1). The first weight loss from the original crystalline sample confirms the presence of the stoichiometric acetonitrile sol-

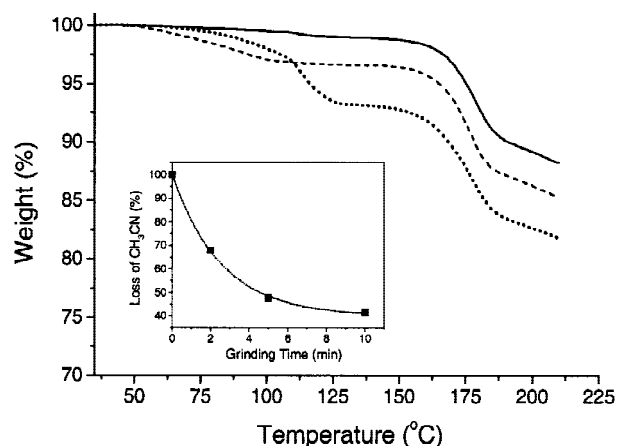


Figure 1. TGA curves of a crystalline QHCl- CH_3CN sample (dotted line), after grinding for 10 min (dashed line) and a sample after heating at 60°C under vacuum for 3 hours (solid line). Inset contains the plot of loss of acetonitrile in QHCl- CH_3CN versus grinding time as described in the text.

vate. The reduced first stage of weight loss for the ground samples and preheated samples indicates partial to total desolvation during those processes. From the crystalline structure of QHCl- CH_3CN , the acetonitrile molecules loosely occupy lattice channels without direct interaction with adjacent units.¹⁹ Thus, the initial loss of solvent at 60°C, well below the boiling point of acetonitrile (82°C), is understandable. When the particle size was further reduced to 1 to 10 μm during grinding, the temperature for initial release of acetonitrile was lowered to about 50°C. The gradual decrease of the acetonitrile content by grinding the crystalline solvate (Fig. 1 inset) was qualitatively correlated to a decreased intensity of the CN absorption peak near 2200 cm^{-1} when the process was also followed using FT-IR measurements. The second weight loss from 150°C to 200°C, which was identical in all samples, corresponds to a weight change expected for the cyclization reaction and the stoichiometric loss of HCl and water (11.5% from theoretical calculations, see Scheme 1). The nearly quantitative transformation from QHCl to DKP under these conditions was further supported by HPLC assay and the absence of Cl^- , as determined by titration with silver nitrate solution.

Formation of Amorphous Quinapril Hydrochloride

Two methods were used to prepare the amorphous form of QHCl in this study. Grinding of the

crystal represents the change from a highly ordered system to a disordered system, whereas solvent evaporation represents the change from a more disordered solution to a less disordered amorphous solid. Both methods gave purely amorphous samples as characterized by a PXRD amorphous halo pattern centered around $20^\circ 2\theta$ and by optical microscopic examination under polarized light.

The formation of amorphous QHCl from grinding of the acetonitrile solvate crystal and subsequent desolvation was monitored by PXRD (Fig. 2) to qualitatively show the gradual transition from the crystalline form to the amorphous form. The intensities of the crystalline peaks of QHCl-CH₃CN decreased with an increase in grinding time, and a halo pattern of the typical amorphous form was observed after 5 minutes of grinding.

The DSC study of the two amorphous QHCl samples exhibited similar glass transitions and heat capacity changes at T_g (Table I). Figure 3 shows a plot of scanning rates used to measure T_g versus the glass transition temperature observed for the amorphous QHCl sample prepared by solvent evaporation. From the slope of the curve, it is possible to evaluate the fragility and related parameters of an amorphous sample.^{20,21}

FT-IR Evaluation

It is apparent from the previous results that the crystalline QHCl acetonitrile solvate is easily converted to the amorphous state via grinding and desolvation. In the crystal structure,¹⁹ quinapril molecules are linked by hydrogen bonds between the amine and the carboxylic acid groups and by chloride ion bridges (Scheme 2). Because these groups might be expected to be affected by the process leading to the amorphous state, FT-IR spectra for QHCl were followed during the various processes used to cause the formation of the amorphous state. The KCl pellet was used because small shifts for some absorption peaks were observed during the preliminary study when the KBr pellet was used. This kind of solid-state anomaly in IR spectra has been reported previously²² and is probably related to metathetical exchange of the halide anions between the compound (Cl⁻) and the matrix (Br⁻). Two regions in the FT-IR spectra were especially sensitive to the processing of QHCl, in that they exhibited a significant systematic shift during the amorphization process. One, as shown in Table II, was the carbonyl functional group region (1600–1800

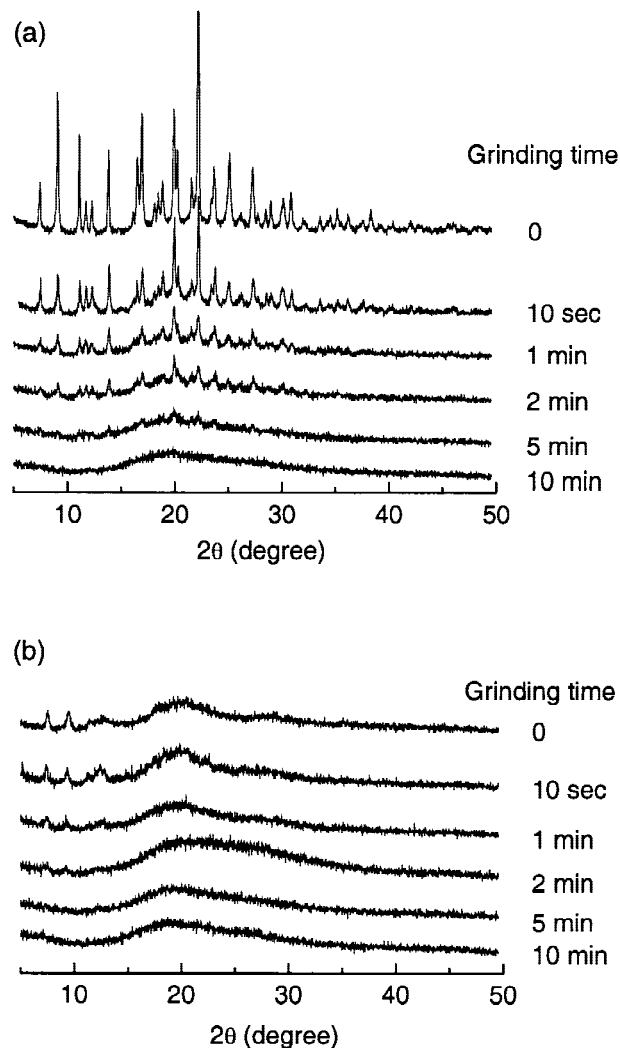


Figure 2. PXRD patterns of samples obtained from grinding of crystalline QHCl-CH₃CN for different time intervals (a) and samples with additional desolvation at 45°C for 24 hours in a vacuum oven after grinding (b).

cm⁻¹). The 1700 to 1750 cm⁻¹ bands represent the overlap of the ester and carboxylic acid C=O stretching vibrations, the change of which is the result of the combination of the weakening or breaking of the hydrogen bonds between the ammonium hydrogen and the neighboring molecule's carboxylic acid oxygen (H_a...O*), as well as possible intramolecular hydrogen bond formation between the ester group and some of those freed H-donor groups (see Scheme 2). The band shift near 1600 cm⁻¹ is attributed to the nonplanar conformation change of the amide bond. The two peaks in the second region at 700 to 800 cm⁻¹ are due to the overlap of out-of-plane aromatic C-H

Table I. DSC Glass Transition Parameters of Two Amorphous Quinapril HCl Samples Prepared by Different Procedures Obtained at a Scanning Rate of 20°C/min

| | Crystal Grinding | Solvent Evaporation |
|--|------------------|---------------------|
| $T_{g(\text{onset})}$ (°C) | 91.3 | 91.7 |
| ΔC_p (JK ⁻¹ g ⁻¹) | 0.41 | 0.40 |

bend or wag vibrations from the mono-substituted and 1,2-substituted benzene rings.²³ After grinding of the crystal for 5 minutes, the two absorption bands at 756 and 709 cm⁻¹ shifted to 748 and 701 cm⁻¹, respectively.

Chemical Degradation of Amorphous Quinapril HCl

Preliminary Studies

To evaluate whether the major cyclization reaction being studied takes place in only an amorphous phase, with the absence of any crystalline forms of either reactant or products that could influence the reaction mechanism, amorphous QHCl was heated at 80°C in a desiccator containing P₂O₅. As shown in Figure 4, after 50% decomposition of amorphous QHCl, the PXRD pattern was still mainly amorphous with only a barely perceptible amount of crystal formation, crystallographically identical to DKP crystal. There

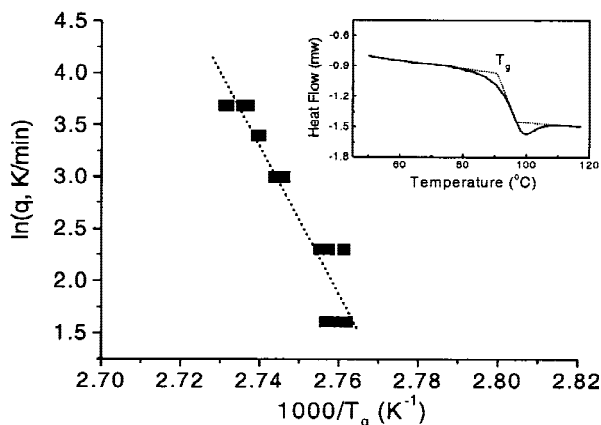
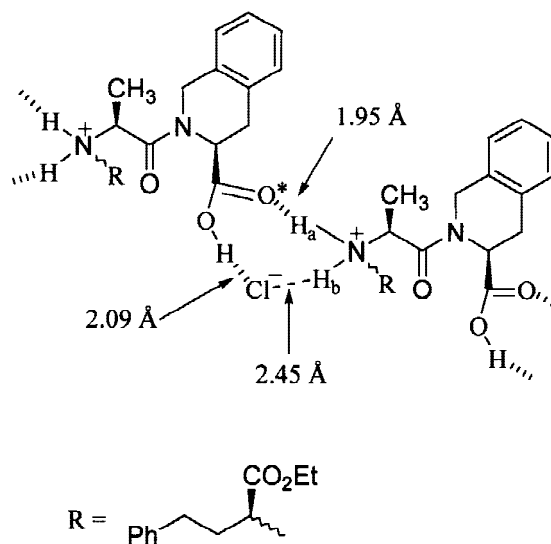


Figure 3. Plot of the natural logarithm of DSC scanning rate (q , K/min) versus the reciprocal of the glass transition temperature for amorphous QHCl samples obtained by solvent evaporation. Inset shows the thermal events associated with a typical glass transition.



were no detectable diffraction peaks caused by any other materials. The amorphous nature of the reaction system over the conditions reported later was also verified at other decomposition temperatures. In all subsequent analyses, we only report kinetic results over the first 15 to 25% of degradation, where the reaction takes place in a one-phase amorphous solid state and is not influenced by any phase transformations. Over this time period it was not possible to establish whether the reaction was first-order or zero-order with respect to the amount of QHCl remaining. We have expressed the reaction in terms of a first-order rate constant in all cases to coincide with its degradation reaction in solution where the first-order kinetics are more obvious. When amorphous samples prepared by grinding were compared with those made by solvent evaporation, chemical reaction rates were essentially the same in all cases.

Chemical Degradation as a Function of Sample Mass

In Figure 5 we show the rate constants of the cyclization reaction of amorphous QHCl samples under the atmosphere created in the closed desiccator containing P₂O₅ at 80°C. The initial weights of these samples ranged from 0.5 to 15 mg, with particle size in the range of 1 to 10 μm. There is a distinct effect of initial weight of samples, the smaller the initial weight the faster the rate of degradation. Included in the inset of Figure 5 are data for the same samples stored at

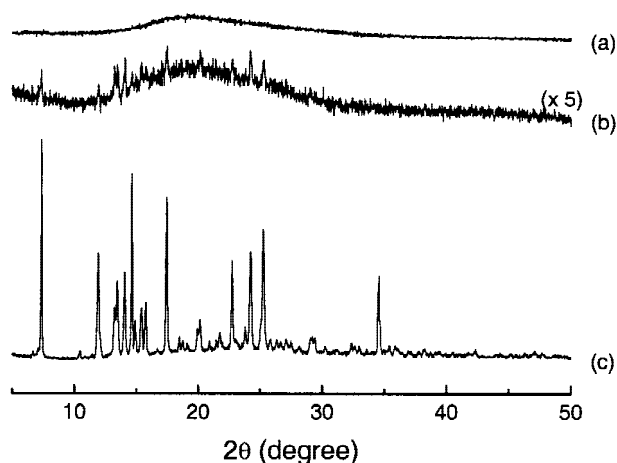
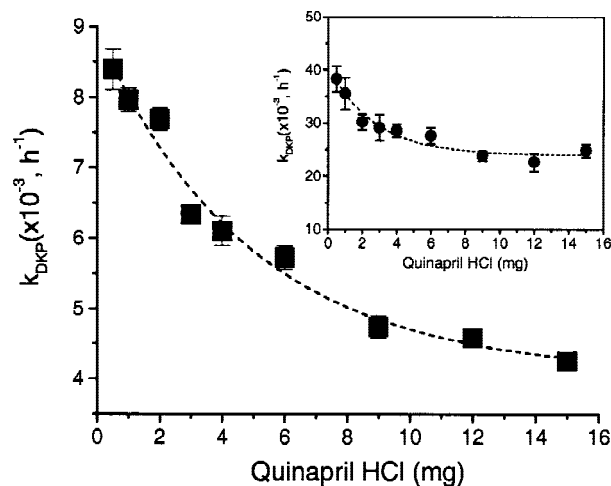
Table II. The FT-IR Shift of Carbonyl Groups in Quinapril HCl with the Formation of the Amorphous State

| | (CO ₂ R, CO ₂ H) 1700 cm ⁻¹ | | (CONR ₂) 1600 cm ⁻¹ |
|--|--|--------|--|
| QHCl-CH ₃ CN crystal | (45.3) | (01.9) | (46.9) |
| Grinding crystal 10 s | (44.3) | (04.8) | (46.9) |
| Grinding crystal 1 min | (41.4) | | (47.9) |
| Grinding crystal 2 min | (40.4) | | (48.8) |
| Grinding crystal 5 min | (40.4) | | (49.8) |
| Grinding, totally amorphous | (39.5) | | (51.7) |
| Solvent evaporation, totally amorphous | (39.5) | | (51.7) |

80°C, but where a vacuum of about 1 torr was applied to the desiccator. Note the roughly doubling (100% change) of the reaction rate going from 15 to 0.5 mg under a dry atmosphere of the closed desiccator, whereas under vacuum at comparable weights the reaction is considerably faster and the change in reaction rate from 15 to 0.5 mg initial weight is significantly less (less than 40%).

Because the cyclization reaction produces two gaseous products, HCl and water, we carried out a study of the degradation of 10 mg amorphous QHCl samples at 80°C in which the reaction con-

tainers within the desiccator were either kept open to the atmosphere (data reported so far) or closed to the atmosphere. If the rate of the release of gaseous products was involved in this reaction, some effects should be observed. Indeed, as shown in Figure 6, the cyclization reaction showed an initially faster rate in the closed system, but the rate slowed considerably at later times. The buildup of water as one of the gaseous products was also reflected on the increased hydrolysis reaction in the closed system, as shown in Figure 6.

**Figure 4.** X-ray powder diffraction pattern of amorphous QHCl after 30% decomposition at 80°C (a), after 50% decomposition at 80°C (the intensity was enlarged five times for clearer comparison) (b), and DKP crystal (c).**Figure 5.** Plot of the effect of sample mass on the cyclization reaction rate constant (k_{DKP}) of amorphous QHCl (made by solvent evaporation) at 80°C. Inset shows the results of the same experiment but conducted under vacuum.

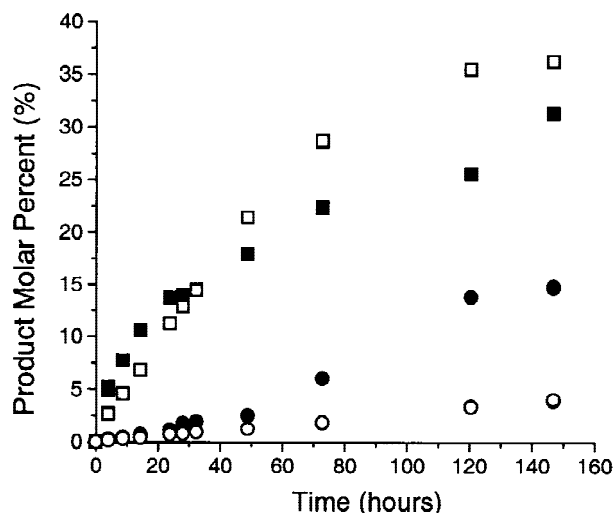


Figure 6. The comparison of cyclization and hydrolysis product formation from the degradation of amorphous QHCl (made by solvent evaporation) at 80°C in open and closed reaction containers. DKP (■ closed, □ open), DA (● closed, ○ open).

Studies with Mixtures

In view of the observed sample mass effects, it was of interest to see whether there would be any effects by diluting the drug with another nonre-active solid. The mixture samples containing various amounts of QHCl were brought up to a constant total weight (i.e., 10 mg, the weight of QHCl mostly used in this study) by solid additives. For this purpose, we chose well-defined glass beads (see experimental section) as materials that would simply keep the particles of QHCl separated by dilution. We also included studies with identical siliconized glass beads to account for the possibility of specific effects from the glass surface, as well as amorphous trehalose, as an example of a typical polar excipient.

As can be seen in Figure 7, for the cyclization reaction, dilution of amorphous QHCl with the various additives produces a change in reaction rate similar to that observed in Figure 5 for changing the mass of drug alone, although the absolute rate constants are different for the same amount of drug in these two situations. The absence of a specific additive effect is seen by the excellent agreement in degradation rates for all three additives at the same weight ratio.

Effect of Temperature

The solid-state degradation of amorphous quinapril HCl, alone and in mixtures under dry

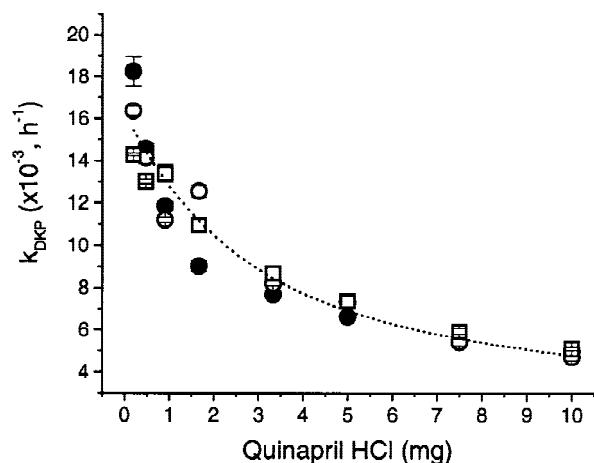


Figure 7. Plots of cyclization reaction rate constants (k_{DKP}) versus amount of amorphous QHCl (made by solvent evaporation) in 10 mg of mixtures with glass beads (●), siliconized glass beads (○), and amorphous trehalose (□) at 80°C.

conditions, was studied at several temperatures from 60°C to 104°C. The Arrhenius plots of the cyclization reaction for 10 mg and 2 mg samples of pure amorphous QHCl and two physical mixtures are shown in Figure 8. There is a distinct break in the plot in the vicinity of T_g for the 10-mg sample, whereas the deviation for the 2-mg sample occurs at a lower temperature. The mixtures, however, exhibit negligible deviation from a straight line over the whole experimental temperature range.

The apparent Arrhenius plot parameters (A and E_a) for the cyclization reaction, obtained from fitting the linear regions of the data in Figure 8, are summarized in Table III. Also included are the activation enthalpy (ΔH^\ddagger) and entropy (ΔS^\ddagger) obtained from Eyring plots based on transition-state theory. The cyclization reaction parameters obtained for the 2-mg sample and the two mixtures are reasonably close, but they are somewhat different from those obtained with the 10-mg samples.

DISCUSSION

Properties of Amorphous Quinapril HCl

The results of this study show that the crystalline QHCl-CH₃CN solvate can easily be rendered fully amorphous by a combination of desolvation and grinding. Amorphous samples made by this method exhibit essentially the same physical and chemical characteristics as samples made by sol-

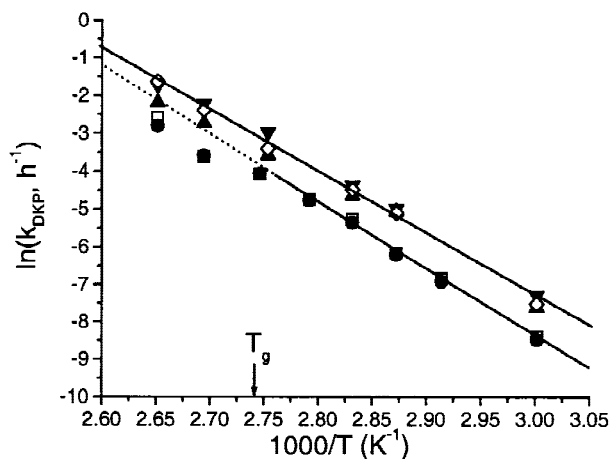


Figure 8. Arrhenius plots of the cyclization reaction for 10 mg samples of amorphous QHCl from grinding (□), 10 mg samples of amorphous QHCl from solvent evaporation (●), 2 mg samples of amorphous QHCl from solvent evaporation (▲), 10 mg samples of an amorphous QHCl-trehalose mixture (▼, 1 : 4, w/w) and of an amorphous QHCl-glass bead mixture (◇, 1:4, w/w).

vent evaporation. The changes of certain functional groups in the FT-IR spectra (Table II) during the formation of the amorphous state, especially groups involved in the hydrogen bonds making up the crystal lattice, indicate why it is relatively easy to create the amorphous state by desolvation and grinding. In particular, the almost complete formation of the amorphous state from the acetonitrile solvate after 5 minutes of grinding [Fig. 2(a)] correlates well to the more than 50% loss of the acetonitrile from the solvate (Fig. 1 inset), whereas a combination of grinding and subsequent desolvation under vacuum can decrease the crystallinity even more efficiently [Fig. 2(b)]. This is most likely due to the extra free volume in the lattice channels created by the removal of the solvent, as observed from the crystal structure.¹⁹ Indeed, as an indication of the strong tendency for this system to be rendered at least partially amorphous by minimal processing, crystalline samples in the acetonitrile solvate form exhibited decreased PXRD peak intensities simply by compressing in a Carver press as shown in Figure 9(b). This partial amorphization was also observed with polarizing microscopy. An even more dramatic loss of crystallinity was observed when the crystalline solvate samples were desolvated under vacuum and then subjected to slight manual pressure during measurement handling [Fig. 9(c)]. Meanwhile, the relatively high glass

transition temperature (for such a small molecule) of the amorphous form and the apparent inability to exist as a nonsolvated crystal⁷ precludes recrystallization of amorphous quinapril HCl under normal storage conditions.

Molecular Mobility and Chemical Reactivity

Although large molecular motions in the solid state, especially for crystalline samples, are generally hindered under pharmaceutical storage conditions, at elevated temperatures and in the amorphous state, molecules can be in a position to acquire sufficient energy and mobility to overcome the energetic barriers. Therefore, it is interesting to compare the reactivity of an amorphous system in this study with those in the crystalline state and in solution. From Table III, the overall activation energy, E_a , for the cyclization reaction of QHCl in the amorphous phase is on the order of 30 to 35 kcal/mol. The activation energy of a similar cyclization reaction in the crystalline state has been shown to be about 60 kcal/mol,²⁴ whereas in solution the value is about 20 kcal/mol.^{8,25} It seems, therefore, that the effect of molecular mobility does play an important role in this type of cyclization reaction.

To evaluate this further, it would be interesting to carry out some assessment of the temperature dependence of the structural relaxation times of amorphous QHCl in the range of temperatures at which chemical reactivity was studied and to see whether the change of reactivity with temperature correlates with the change in molecular mobility. Because of the relatively low chemical stability of amorphous QHCl even below its T_g , it was not possible to carry out long-term direct measurements of relaxation time, τ , by thermomechanical, dielectric, or thermal methods, as is often done with amorphous materials. However, it is possible to characterize relaxation times in an approximate manner by simply measuring T_g as a function of scanning rate in the DSC and carrying out an analysis proposed by Moynihan et al.²⁶ and recently evaluated and validated for an organic molecule with amorphous indomethacin.²⁷

Thus, from a plot of the logarithm of the DSC scanning rate, $\ln|q|$, versus T_g , as shown in Figure 3, the activation energy for enthalpy relaxation (ΔH^*), can be obtained by applying eq. 1.

$$\frac{d(\ln|q|)}{d(1/T_g)} = -\frac{\Delta H^*}{R} \quad (1)$$

Table III. Summary of the Kinetic Parameters from Arrhenius Plots for the Cyclization Reaction of Pure Amorphous Quinapril HCl and Some Mixtures

| | lnA | E _a | ΔH‡ | ΔS‡ (cal/mol K) |
|------------------------------|------------|----------------|------------|-----------------|
| 10 mg QHCl ^a | 44.8 ± 1.8 | 35.5 ± 1.1 | 34.7 ± 0.6 | 12.3 ± 1.8 |
| 2 mg QHCl ^b | 37.4 ± 2.0 | 29.7 ± 1.4 | 29.4 ± 1.6 | 15.1 ± 4.5 |
| QHCl-trehalose ^c | 39.9 ± 1.1 | 31.3 ± 0.8 | 31.2 ± 1.1 | 9.4 ± 3.2 |
| QHCl-glass bead ^c | 41.4 ± 1.2 | 32.4 ± 0.9 | 32.0 ± 0.9 | 7.5 ± 2.5 |

^a Amorphous quinapril HCl samples from grinding of crystal and solvent evaporation. Parameters were obtained by least-squares linear fitting of the data (□, ●) below T_g in Figure 16.

^b Amorphous quinapril HCl samples from solvent evaporation.

^c Physical mixtures (1:4, w/w) of amorphous quinapril HCl (from solvent evaporation) and additives. Total mass of each sample = 10 mg.

For conditions used in this study, ΔH* can be used as the activation energy for viscous flow (ΔH_η*) to calculate the “fragility parameter” *m*, (eq. 2) and “strength parameter” (*D*, eq. 3).

$$m = \frac{\Delta H_{\eta}^*}{2.303RT_g} \quad (2)$$

$$D = \frac{2.303(m_{\min})^2}{m - m_{\min}} \quad (3)$$

In eq. 3, *m*_{min} = log(τ_{T_g}/τ₀), which takes the value of 16 because the relaxation time at T_g (τ_{T_g}) is usually about 100 sec²⁸ and τ₀ is the relaxation time at the high temperature limit, which is on the order of vibrational lifetimes (≈ 10⁻¹⁴ sec). The parameters obtained for amorphous QHCl were:

ΔH* = 141 ± 11 kcal/mol, *m* = 85 ± 7, *D* = 8.5 ± 1.0, which indicate that amorphous QHCl is a relatively fragile glass near its glass transition temperature. The ideal glass transition temperature T₀, which is thought to mark the point of zero configurational entropy,⁶ was calculated to be 296 K (23°C) from eq. 4.

$$T_0 = T_g \left(1 - \frac{m_{\min}}{m} \right) \quad (4)$$

From the fragility parameters obtained in the preceding, the relaxation times of amorphous QHCl above its glass transition temperature can be estimated by using the Vogel-Tammann-Fulcher (VTF) equation²⁸ as shown in eq. 5.

$$\tau = \tau_0 \exp\left(\frac{DT_0}{T - T_0}\right) \quad (5)$$

Because the VTF equation assumes the amorphous state to be an equilibrium super-cooled liquid at all temperatures, it has been shown that it tends to predict much higher relaxation times at temperatures less than T_g than actually occur in the glassy state.^{29,30} To better estimate relaxation times at temperatures less than T_g, in the glassy state, therefore, it is more appropriate to combine the Adam-Gibbs equation with the VTF equation to give eq. 6, the Adam-Gibbs-Vogel (AGV) equation.²⁹

$$\tau = \tau_0 \exp\left(\frac{DT_0}{T(1 - T_0/T_f)}\right) \quad (6)$$

In eq. 6, T_f, the fictive temperature, is defined as the temperature at which the nonequilibrium value of some macroscopic property would be the equilibrium one predicted from the VTF equation.

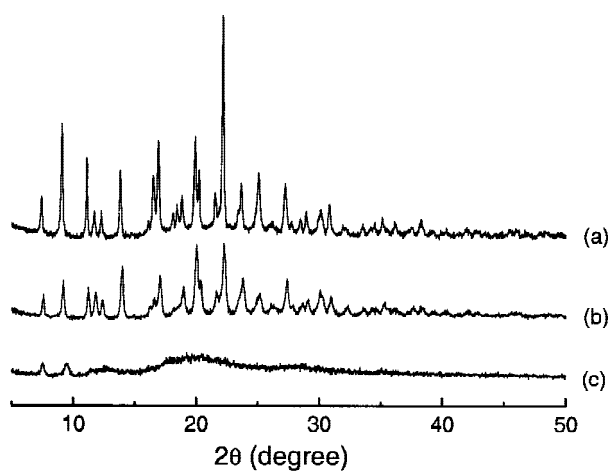


Figure 9. PXRD of crystalline QHCl-CH₃CN (a), sample after compression using a Carver press (~10⁴ lb/cm²) (b), and sample after desolvation under vacuum at 45°C for 24 hours (c).

In the equilibrium state above T_g , T_f is equal to T , and eq. 6 is identical to eq. 5. For the purpose of this approximate analysis below T_g , we follow the practice of assuming that a good estimate of T_f immediately after the formation of the glass is T_g .³¹ Therefore in Figure 10, the solid and dotted lines represent predictions of $\log(\tau)$ versus T/T_g , assuming the values of D , T_0 , and τ_0 presented earlier.

Molecular mobility that might influence a chemical reaction can involve translational or rotational motions of entire molecules or intramolecular motions involving specific portions of the molecule. The translational and rotational motions of most molecules in single- or multiple-component systems, as reflected in the diffusion coefficient, are generally coupled to shear viscosity, η . For example, the relationship between the translational diffusion coefficient (D_r) and shear viscosity (η) is given by the Stokes-Einstein equation:

$$D_r = \frac{k_B T}{6\pi\eta r} \quad (7)$$

where r is the molecular radius, k_B is the Boltzmann constant, and T is temperature. The viscosity (η) is a measure of the liquid response to a suddenly imposed shear stress and is proportional to the corresponding relaxation time (τ) by the Maxwell equation.³² Because the rate constant (k) for a molecular mobility-controlled reaction is proportional to the diffusion coefficient D_r ,^{33,34} reaction rate constants at a constant temperature can be correlated to the ratio of their relaxation times, τ , as shown in eq. 8:

$$\frac{k_2}{k_1} \approx \frac{D_{r2}}{D_{r1}} \approx \left(\frac{\eta_1}{\eta_2}\right)^\xi \approx \left(\frac{\tau_1}{\tau_2}\right)^\xi \quad (8)$$

where ξ is introduced, for amorphous materials near the glass transition temperature, to compensate for any "decoupling" between measured diffusion coefficient values and prediction from viscosity and reorientational relaxation.³⁴

If we wish to examine the ratio of k_1 to k_2 for the same reaction at different temperatures (T_1/T_2), then

$$\frac{k_2}{k_1} \approx \frac{D_{r2}}{D_{r1}} \approx \left(\frac{T_2}{T_1}\right) \left(\frac{\tau_1}{\tau_2}\right)^\xi \quad (9)$$

If we assume that the solid-state cyclization reaction of amorphous QHCl is controlled by mo-

lecular mobility and the relaxation time (τ) at the glass transition temperature for this system is 100 sec,²¹ by comparing the reaction rate constant at T_g relative to those at other temperatures and applying eq. 9, we should be able to calculate the corresponding expected equivalent relaxation times at the different experimental temperatures. In Figure 10 the data points represent the relaxation times calculated from rate constants for the cyclization reaction with $\xi = 1$ (complete coupling between D and τ) and 0.75 (incomplete coupling between D and τ as suggested by Fujara et al.³⁴), compared with predictions from the VTF and AGV equations at temperatures greater than and less than T_g , respectively. Below T_g , the change in relaxation times obtained from observed reaction constants appears to correlate quite well with the AGV equation prediction. Above T_g , the estimates of τ from reaction rates are greater (slower reaction rate) than predicted from the VTF equation.

In Scheme 3 we show a simplified mechanistic scheme for the cyclization reaction of quinapril hydrochloride. There are basically three steps in this reaction that could act as activation barriers and, hence, contribute to the apparent overall reaction rate: (i) proton transfer to form HCl and the diffusion of HCl gas away from the reaction site; (ii) transformation of the *trans* amide conformation to the *cis* conformation, necessary to bring the nucleophilic amine in proximity to the carboxylic acid group; and (iii) the intramolecular nu-

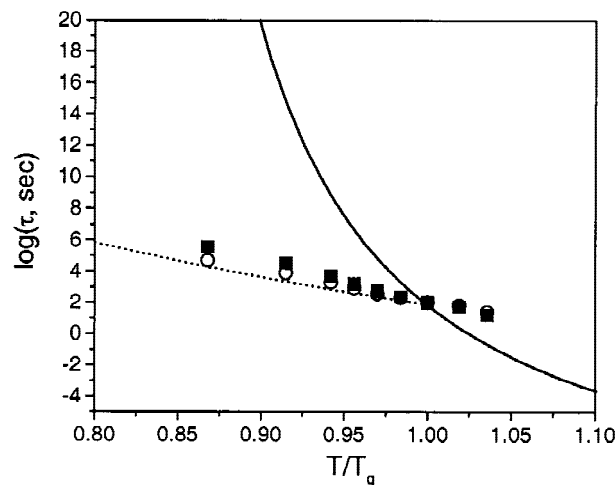
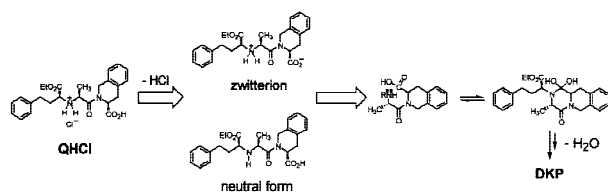


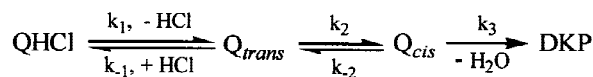
Figure 10. Relaxation times calculated from rate constants for the cyclization reaction from eq. 9 with $\xi = 1$ (\circ) and $\xi = 0.75$ (\blacksquare), respectively. The lines are relaxation time versus temperature predictions using the VTF equation (solid line) and the AGV equation (dotted line), as described in the text.



cleophilic addition, the subsequent breakdown of the tetrahedral intermediate to form the DKP product plus a molecule of water, and the diffusion of water from the reaction site.

In the solution state, we would expect that proton transfer to yield the zwitterionic form of quinapril would occur rapidly.³⁵ The *trans-cis* amide conformation transformation, as shown earlier in some *N*-acyl-proline systems,^{36,37} has an activation energy of about 20 kcal/mol in aqueous solutions.³⁸⁻⁴⁰ This kind of *trans-cis* amide conformational change has been suggested as the rate-limiting step for some protein denaturation reactions in aqueous solution.⁴¹ The intramolecular nucleophilic addition and breakdown of the tetrahedral intermediate in other similar reactions has been suggested to be the rate-limiting step on the basis of analyses of pH effects in aqueous solution.^{42,43}

In the solid state, all three steps would appear to require a critical amount of translational and/or rotational diffusion. From the crystal structure of the QHCl acetonitrile solvate (see Scheme 2), we see that Cl⁻ is hydrogen bonded to the hydrogen atoms of the amine and carboxylic acid groups of two neighboring molecules, which could be carried over to the amorphous phase, at least to some extent. Hence, theoretically, proton transfer to the Cl⁻ to form HCl gas can occur either by way of the amine to produce the neutral form or by way of the carboxylic acid to produce the zwitterionic form during thermal treatment (see Scheme 3). In either case, significant molecular mobility is required to form the covalent H-Cl bond (bond length 1.28 Å) and to simultaneously break an O-H or N-H bond. The HCl molecules produced, which might still be hydrogen-bonded to quinapril molecules, need to overcome another energetic barrier to escape from the solid matrix to the vapor state. If HCl molecules do not have sufficient mobility to escape, the time scale might be enough for the reverse reaction (see Scheme 4), which will result in decreased overall degradation rates. In a similar situation the thermal decomposition of certain solid alkylammonium chlorides at high temperature exhibits an activation energy



of about 30 to 40 kcal/mol,⁴⁴ consistent with values obtained for the present system.

Meanwhile, from the crystal structure of QHCl-CH₃CN,¹⁹ the amide bond is predominantly in the *trans* conformation. Because of the possible larger steric effect from the 1,2,3,4-tetrahydro-3-isoquinolinecarboxylic acid group, we expect that the *trans-cis* transformation barrier in the solid state should be higher than 20 kcal/mol. Therefore, the *trans-cis* conformation change, another prerequisite for the cyclization reaction, should also require significant molecular mobility. The FT-IR studies reported earlier (Table II) indicate a nonplanar amide conformation change during the formation of the amorphous form. This probably, in part, will contribute to the increased molecular mobility and chemical reactivity in the amorphous state compared with the crystalline state.

To assess the possible roles of each of these steps and other variables on the overall cyclization reaction, we can carry out the following analysis. We can first assume that any reaction of HCl with the *cis*-quinapril (Q_{cis}) is insignificant, which would be very likely if the HCl molecules already had enough time to escape from the reaction site or if the conformational change to the *cis* form might cause the basic groups of quinapril to be inaccessible to HCl. Then the reaction in Scheme 3 can be quantitatively expressed as Scheme 4, where *k*₁, *k*₂, and *k*₃ are the three forward reaction rate constants and *k*₋₁ and *k*₋₂ are those of the first two reverse reactions. The possible reaction between DKP and water is ignored in the solid state because some of the representative hydrolysis products from DKP in aqueous solution are not detected in this study when the open vials in a desiccator containing P₂O₅ are used.

By assuming the steady-state approximation⁴⁵ for both quinapril forms (Q_{trans} and Q_{cis}), it can be shown that

$$\frac{d[\text{Q}_{\text{trans}}]}{dt} = k_1[\text{QHCl}] + k_{-2}[\text{Q}_{\text{cis}}] - k_{-1}[\text{Q}_{\text{trans}}]P_{\text{HCl}} - k_2[\text{Q}_{\text{trans}}] \approx 0 \quad (10)$$

and

$$\frac{d[Q_{\text{cis}}]}{dt} = k_2[Q_{\text{trans}}] - k_{-2}[Q_{\text{cis}}] - k_3[Q_{\text{cis}}] \approx 0 \quad (11)$$

Then from Scheme 4 the observed rate constant for the formation of DKP (k_{obs}) can be expressed as eq. 12.

$$k_{\text{obs}} = \frac{k_1 k_2 k_3}{k_2 k_3 + k_{-1}(k_3 + k_{-2})P_{\text{HCl}}} \quad (12)$$

Eq. 12 shows the combined contributions from each step in the reaction scheme and in particular the adverse effect of any local partial pressure buildup of HCl gas (P_{HCl}) on the overall reaction rate.

Effects of Particle Morphology

The observed significant effects of sample weight on the degradation rate strongly imply that additional factors associated with the physical characteristics of the solid state are contributing to the observed kinetics. All results indicate that the restriction of gases to escape from the reaction matrix tends to slow down the reaction significantly, whereas the reaction rate increases when gas removal is facilitated by applying a vacuum (Fig. 5). On the basis of the significant differences in measured reaction rates for sample weights ranging from 0.5 to 15 mg, we would hypothesize that in some manner this might be due to a limitation on the rate of removal of HCl gas from inside the solid matrix and hence a slowdown of the overall reaction rate by increasing the reverse reaction of the first step as discussed previously. We might ask how would sample weight affect removal of HCl gas? This effect is probably due to the tendency for amorphous QHCl particles to soften (lower viscosity) near and above its T_g of about 91°C. The particles most likely soften even more as the reaction proceeds because the major degradation product, amorphous DKP, has a glass transition temperature of about 37°C as measured by DSC at 20K/min and any water present can also act as a plasticizer.⁶ Such a loss in viscosity in addition to increased molecular mobility might be expected to lead to a coalescence of particles into a larger mass with a reduced surface/volume ratio. This, in turn, could lead to a reduced rate of HCl diffusion out of the solid because of less exposed surface. This hypothesis is supported by the observation of an approximately

100% decrease of degradation rate for samples of larger particle size (500–1000 μm) relative to that of small particle size (1–10 μm) samples having the same total weight (data not shown). Significant coalescence of particles after storage at 80°C for 70 hours was observed by SEM as shown in Figure 11(a) and (b). Coalescence became particularly severe when samples were stored at temperatures greater than T_g , as could be observed by optical microscopy and even visually. To further test this hypothesis, we intentionally produced large-scale agglomeration by annealing amorphous QHCl samples at 100°C for a brief time. As shown in Figure 12, this sample exhibited a significantly slower degradation rate than that of untreated samples despite a small amount of initial degradation caused by the initial heating at 100°C; the degradation rate of untreated samples is about two times that of the rate of annealed samples, a difference that correlates well with the sample weight experiment (Fig. 5) and the particle size experiment. Such an interpretation based on a reduced surface/volume ratio appears to be consistent with an earlier study of the solid-state decomposition of CaCO_3 to yield the CO_2 gas, in which a pelleted system was much less reactive than the powdered form,⁴⁶ presumably because of slowing of CO_2 transport and release.

Dilution of the drug particles by mixing with another solid such as the glass beads and treha-

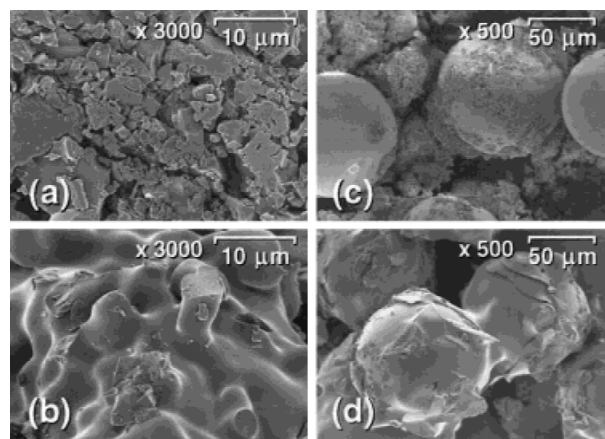


Figure 11. SEM images of the original amorphous QHCl from solvent evaporation (a), and a sample after storage at 80°C for 70 hours in a desiccator (20% decomposition) (b), physical mixture of amorphous QHCl with siliconized glass beads (1:5, w/w) (c), and after storage at 80°C for 40 hours in a desiccator (30% decomposition) (d).

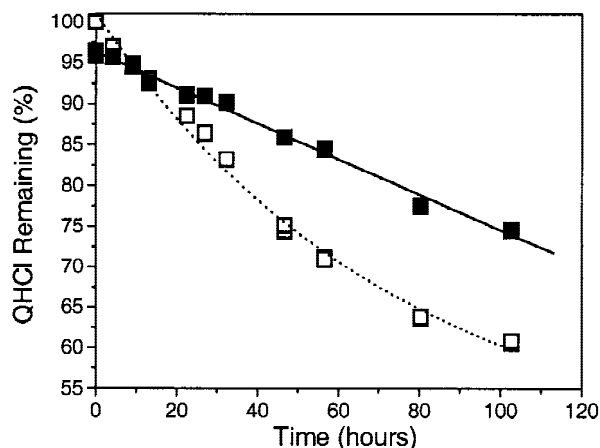


Figure 12. Degradation (at 80°C) of amorphous quinapril hydrochloride samples (10 mg) annealed at 100°C for 5 min (■) and same amount of untreated samples (□).

lose most likely prevents large-scale aggregation of QHCl particles and hence prevents the slowing down of HCl release. On the other hand, local agglomeration of drug particles is still observed, depending on the ratio of drug to additive in the mixture and their particle size difference. As shown in Figure 11 (c) and (d), for the mixtures of amorphous QHCl and siliconized glass beads, this local agglomeration occurs on the surface of glass beads, appearing to form a drug "film" after heating. We would conclude, therefore, that the rate of HCl diffusion is affected by both the exposed surface area and the thickness of the drug film. When the additive ratio in the mixture increases, the exposed drug surface increases while the thickness of the drug layer decreases, both favoring the diffusion of HCl gas and increasing the rate of the overall reaction. Note in this regard the larger degradation rate constants of QHCl in mixtures (Fig. 7) than those of the same amounts of pure drug (Fig. 5). This hypothesis also agrees well with the observed small but significant discontinuities in the Arrhenius plots of Figure 8 for the pure samples at high temperatures, in which softening of the system should be enhanced. On the other hand, no significant effects were observed when the drugs were diluted with the glass beads and trehalose. Such significant softening and agglomeration above T_g with a resulting slowing down of the reaction may also contribute, at least partially, to the relatively poor predictions above T_g in Figure 10, in which the predicted molecular mobilities from the chemical reaction rates are much slower than those pre-

dicted by the VTF relaxation time obtained from the scanning rate dependency of T_g .

CONCLUSIONS

Crystalline QHCl can be easily rendered amorphous by desolvation of the crystalline acetonitrile solvate and mechanical grinding. The amorphous form, also prepared by evaporation from a CH_2Cl_2 solution, has a glass transition temperature of 91°C and can be considered a fairly fragile material with a D parameter of 8.5 and a T_0 of 23°C. The molecular level disorder in QHCl, as indicated by FT-IR spectra analysis, correlates to the mobility of several functional groups in the amorphous state. Amorphous QHCl readily undergoes a cyclization reaction to form the corresponding DKP under dry conditions over the temperature range of 60 to 104°C with an apparent activation energy of about 30 to 35 kcal/mol. The cyclization reaction involves three possible energetic barriers, including the production of two gaseous products, HCl and H_2O , that can be affected by the molecular mobility of the amorphous state. A good correlation between relative reaction rate constants and structural relaxation time was obtained below T_g , but above T_g , despite shorter predicted relaxation times, the reaction rates were greatly reduced. The reduced surface/volume ratio caused by agglomeration and sintering of QHCl particles during heating, and a slower rate of HCl gas removal, appear responsible for the decreased reaction rate and the observed effects of sample-related variables.

This complexity with regard to morphologic changes, and the possible rate-determining diffusion of HCl gas, makes quantitative evaluation of the kinetic model, expressed by equation 10, very difficult and more probing of this system will be required to do so.

ACKNOWLEDGMENTS

This study was supported by the Purdue-Wisconsin Joint Program on the Physical and Chemical Stability of Pharmaceutical Solids. Dr. Richard Noll from the Material Science Center, University of Wisconsin-Madison, is acknowledged for the technical assistance with the SEM measurement. We are grateful to the Department of Chemical Engineering, University of Wisconsin-Madison, for use of the FT-IR and TGA equipment.

REFERENCES

- Paul IC, Curtin DY. 1973. Thermal induced organic reactions in the solid state. *Acc Chem Res* 6:217-225.
- Byrn SR. 1982. *Solid state chemistry of drugs*, 1st ed. New York: Academic.
- Pikal MJ, Lukes AL, Lang, JE, Gaines K. 1978. Quantitative crystallinity determinations for beta-lactam antibiotics by solution calorimetry: correlations with stability. *J Pharm Sci* 67:767-773.
- Oberholtzer ER, Brenner GS. 1979. Cefoxitin sodium: solution and solid-state chemical studies. *J Pharm Sci* 68:863-866.
- Oguchi T, Yonemochi E, Yamamoto K, Nakai Y. 1989. Freeze-drying of drug additive binary-systems. 2. Relationship between decarboxylation behavior and molecular states of *P*-aminosalicylic acid. *Chem Pharm Bull* 37:3088-3091.
- Hancock BC, Zografi G. 1997. Characteristics and significance of the amorphous state in pharmaceutical systems. *J Pharm Sci* 86:1-12.
- Xu W. August 1997. Investigations of solid-state stability of selected bioactive compounds. Ph.D. Thesis. West Lafayette, IN: Purdue University.
- Gu L, Strickley RG. 1987. Diketopiperazine formation, hydrolysis, and epimerization of the new dipeptide angiotensin-converting enzyme inhibitor RS-10085. *Pharm Res* 4:392-397.
- Cotton ML, Wu DW, Vadas EB. 1987. Drug-excipient interaction study of enalapril maleate using thermal analysis and scanning electron microscopy. *Int J Pharm* 40:129-142.
- Steinberg SM, Bada JL. 1983. Peptide decomposition in the neutral pH region via the formation of diketopiperazines. *J Org Chem* 48:2295-2298.
- Goolcharran C, Borchardt RT. 1998. Kinetics of diketopiperazine formation using model peptides. *J Pharm Sci* 87:283-288.
- Kertscher U, Bienert M, Krause E, Sepetov NF, Mehlis B. 1993. Spontaneous chemical degradation of substance P in the solid phase and in solution. *Int J Pept Protein Res* 41:207-221.
- Battersby JE, Hancock WS, Canova-Davis E, Oeswein J, O'Connor B. 1994. Diketopiperazine formation and N-terminal degradation in recombinant human growth hormone. *Int J Pept Protein Res* 44:215-222.
- Gisin BF, Merrifield RB. 1972. Carboxyl-catalyzed intramolecular aminolysis. A side reaction on solid-phase peptide synthesis. *J Am Chem Soc* 94:3102-3106.
- Goel OP, Krolls J. U. S. Patent 4,761,476, August 2, 1988.
- Klutchko S, Blankley CJ, Fleming RW, Hinkley JM, Werner AE, Nordin I, Holmes A, Hoefle ML, Cohen DM, Essenburg AD, Kaplan HR. 1986. Synthesis of novel angiotensin converting enzyme inhibitor quinapril and related compounds. A divergence of structure-activity relationships for non-sulfhydryl and sulfhydryl types. *J Med Chem* 29:1953-1961.
- Yang YW. August 1985. Capillary flow phenomena as related to wettability in porous media. Ph.D. Thesis. Madison, WI: University of Wisconsin-Madison.
- Saleki-Gerhardt A, Zografi G. 1994. Non-isothermal and isothermal crystallization of sucrose from the amorphous state. *Pharm Res* 11:1166-1173.
- Hausin RJ, Coddling PW. 1991. Molecular and crystal structures of MDL27,467A hydrochloride and quinapril hydrochloride, two ester derivatives of potent angiotensin converting enzyme inhibitors. *J Med Chem* 34:511-517.
- DeBolt M, Esteal A, Macedo P, Moynihan C. 1976. Analysis of structural relaxation in glass using rate heating data. *J Am Ceram Soc* 59:16-21.
- Andronis V, Zografi G. 1998. The molecular mobility of supercooled amorphous indomethacin as a function of temperature and relative humidity. *Pharm Res.* 15:835-841.
- Mutha SC, Ludemann WB. 1976. Solid-state anomalies in IR spectra of compounds of pharmaceutical interest. *J Pharm Sci* 65:1400-1403.
- Nakanishi K, Solomon PH. 1977. *Infrared absorption spectroscopy*, 2nd ed. San Francisco, CA: Holden-Day.
- Leung SS, Grant JW. 1997. Solid state stability studies of model dipeptides: aspartame and aspartylphenylalanine. *J Pharm Sci* 12:305-308.
- Straub JA, Akiyama A, Parmar P, Musso GF. 1995. Chemical pathways of degradation of bradykinin analog, RMP-7. *Pharm Res* 12:305-308.
- Moynihan CT, Easteal AJ, Wilder J, Tucker J. 1974. Dependence of glass transition temperature on heating and cooling rate. *J Phys Chem* 78:2673-2677.
- Andronis V, Zografi G. 1997. Molecular mobility of supercooled amorphous indomethacin; determined by dynamic mechanical analysis. *Pharm Res.* 14:410-414.
- Bohmer R, Ngai KL, Angell CA, Plazek DJ. 1993. Nonexponential relations in strong and fragile glass formers. *J Chem Phys* 99:4201-4209.
- Hodge IM. 1994. Enthalpy relaxation and recovery in amorphous materials. *J Non-Cryst Solids* 169:211-266.
- Hodge IM. 1995. Physical aging in polymer glasses. *Science* 267:1945-1947.
- Scherer GW. 1990. Theories of relaxation. *J Non-Cryst Solids* 123:75-89.
- Angell CA. 1995. Formation of glasses from liquids and biopolymers. *Science* 267:1924-1935.
- Rice SA. 1985. *Comprehensive chemical kinetics*. In: Bamford CH, Tipper CFH, Campton RG, edi-

- tors. Diffusion-limited reactions. Vol 25. Amsterdam: Elsevier.
34. Fujara F, Geil B, Sillescu H, Fleischer G. 1992. Translational and rotational diffusion in supercooled orthoterphenyl close to the glass transition. *Z Phys B: Condensed Matter* 88:195–204.
 35. Horne RA, Axelrod EH. 1964. Proton mobility and electron exchange in aqueous media. *J Chem Phys* 40:1518–1522.
 36. Moore JAW, Jorgenson JW. 1995. Resolution of cis and trans isomers of peptides containing proline using capillary zone electrophoresis. *Anal Chem* 67:3464–3475.
 37. Eberhardt ES, Loh SN, Hinck AP, Raines RT. 1992. Solvent effects on the energetics of prolyl peptide bond isomerization. *J Am Chem Soc* 114:5437–5439.
 38. Roques BP, Garbay-Jaureguiberry C, Combrisson S, Oberlin R. 1977. Determination of rates and barriers to conformational isomerization in the dipeptide L-Pro-L-4Hyp by direct ^{13}C NMR thermal equilibration. *Biopolymers* 16:937–944.
 39. Cheng HN, Bovey FA. 1977. Cis-trans equilibrium and kinetic studies of acetyl-L-proline and glycyl-L-proline. *Biopolymers* 16:1465–1472.
 40. Fischer S, Dunbrack JRL, Karplus M. 1994. Cis-trans imide isomerization of the proline dipeptide. *J Am Chem Soc* 116:11931–11937.
 41. Brandts JF, Halvorson HR, Brennan M. 1975. Consideration of the possibility that the slow step in protein denaturation reactions is due to cis-trans isomerism of proline residues. *Biochem* 14:4953–4963.
 42. Camiller P, Ellul R, Kirby A, Mujahid TG. 1979. The spontaneous formation of amides. The mechanism of lactam formation from 3-(2-amino-phenyl)propionic acid. *J Chem Soc Perkin Trans II* 1617–1620.
 43. Strickley RG, Visor GC, Lin L, Gu L. 1989. An unexpected pH effect on the stability of moexipril lyophilized powder. *Pharm Res* 6:971–975.
 44. Blazejowdki J. 1983. Thermal properties of amine hydrochlorides. Part I. Thermolysis of primary N-alkylammonium chlorides. *Thermochimica Acta* 68:233–260.
 45. Lowry TH, Richardson KS. 1981. Mechanism and theory in organic chemistry, 2nd ed. New York: Harper & Row.
 46. Sharp JH, Wentworth SA. 1969. Kinetic analysis of thermogravimetric data. *Anal Chem* 41:2060–2062.